

# Peptidyl Boronates Inhibit *Salmonella enterica* serovar Typhimurium Lon Protease by a Competitive ATP-Dependent Mechanism<sup>†</sup>

Hilary Frase and Irene Lee\*

Department of Chemistry, Case Western Reserve University, Cleveland, Ohio 44106

Received February 8, 2007; Revised Manuscript Received March 29, 2007

**ABSTRACT:** Lon is a homo-oligomeric ATP-dependent serine protease that functions in the degradation of damaged and certain regulatory proteins. This enzyme has emerged as a novel target in the development of antibiotics because of its importance in conferring bacterial virulence. In this study, we explored the mechanism by which the proteasome inhibitor MG262, a peptidyl boronate, inhibits the peptide hydrolysis activity of *Salmonella enterica* serovar Typhimurium Lon. In addition, we synthesized a fluorescent peptidyl boronate inhibitor based upon the amino acid sequence of a product of peptide hydrolysis by the enzyme. Using steady-state kinetic techniques, we have shown that two peptidyl boronate variants are competitive inhibitors of the peptide hydrolysis activity of Lon and follow the same two-step, time-dependent inhibition mechanism. The first step is rapid and involves binding of the inhibitor and formation of a covalent adduct with the active site serine. This is followed by a second slow step in which Lon undergoes a conformational change or isomerization to increase the interaction of the inhibitor with the proteolytic active site to yield an overall inhibition constant of 5–20 nM. Although inhibition of serine and threonine proteases by peptidyl boronates has been detected previously, Lon is the first protease that has required the binding of ATP in order to observe inhibition.

The emergence of new strains of antibiotic resistant bacteria requires the development of novel therapeutics to treat them. Studies aimed at identifying proteins necessary for bacterial virulence have implicated the importance of Lon protease (1, 2). Pathogenic *Salmonella enterica* are responsible for causing a range of human diseases from mild gastroenteritis (serovar Typhimurium and serovar Enteritidis) to typhoid fever (serovar Typhi). It has been shown that *Salmonella enterica* serovar Typhimurium (*S. Typhimurium*) Lon protease activity is required for systemic infection in mice, a common study model for *S. Typhi* infection in humans (2). In fact, Lon-deficient *S. Typhimurium*, when administered as an oral vaccine to mice, conferred subsequent protection against infection by virulent *S. Typhimurium* (3). Taken together, these studies highlight this enzyme as an

important target in the development of novel therapeutic agents.

Lon, also known as the protease La, is a member of the AAA<sup>+</sup> superfamily (ATPases Associated with different cellular Activities) along with other ATP<sup>1</sup>-dependent proteases, such as ClpXP, HslUV, and the proteasome (4, 5). It is a homo-oligomeric ATP-dependent serine protease that functions in the degradation of damaged and certain short-lived regulatory proteins (6–15). Homologues exist ubiquitously in nature; however, they localize to the cytosol in prokaryotes and to the mitochondrial matrix in eukaryotes (9, 16, 17). Sequence alignment of the human, *Escherichia coli* (*E. coli*), and *S. Typhimurium* Lon proteases has revealed that the bacterial enzymes share greater than 99% sequence identity, but only 42% identity with their human homologue (18). Not surprisingly, the peptide substrate specificity of the bacterial and human Lon proteases differ; however, their ATP hydrolysis activities are kinetically indistinguishable (19).

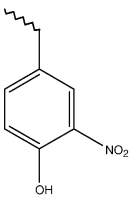
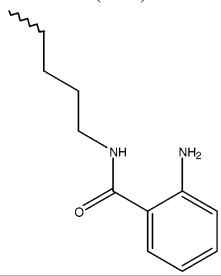
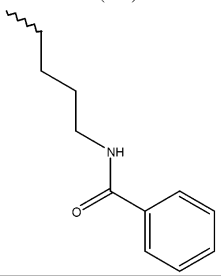

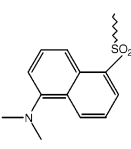
The mechanism by which Lon recognizes a protein substrate or utilizes the energy from ATP hydrolysis to catalyze protein degradation is not well understood. The *E. coli* homologue has long been used as a model for elucidating the molecular details of these processes. Crystallographic studies of a truncated *E. coli* Lon mutant have suggested that this protease utilizes a Ser-Lys dyad to catalyze peptide bond hydrolysis (20, 21). It has also been shown that the *E. coli* enzyme requires only the binding, but not hydrolysis, of ATP in order to cleave a peptide substrate, albeit at a reduced rate (22). Upon ATP binding, the enzyme undergoes a conformational change, which has been suggested to result in the productive alignment of the active site residues for

<sup>†</sup> This work was support by NIH grant GM067172.

\* Corresponding author: Phone: 216-368-6001. Fax: 216-368-3006. E-mail: irene.lee@case.edu.

<sup>1</sup> Abbreviations: ATP, adenosine triphosphate; AMPPNP, adenosine 5'-( $\beta,\gamma$ -imino)triphosphate; ADP, adenosine diphosphate; DTT, dithiothreitol; Abz, anthranilamide; Bz, benzoic acid amide; Abu, 2-aminobutyric acid; 3-NO<sub>2</sub>, 3-nitro; Alloc, allyloxycarbonyl; HBTU, *O*-benzotriazole-*N,N,N',N'*-tetramethyl-uronium-hexafluoro-phosphate; THF, tetrahydrofuran; LDA, lithium diisopropylamide; KHMDS, potassium bis-(trimethylsilyl) amide; TMS, trimethylsilyl; EDC, 1-ethyl-3-[3-dimethylaminopropyl]carbodiimide; TFE, trifluoroethanol; TIS, triisopropylsilane; TFA, trifluoroacetic acid; Pbf, 2,2,4,6,7-pentamethyldihydrobenzofuran-5-sulfonyl; Trt, trityl; Tris, 2-amino-2-(hydroxymethyl)-1,3-propanediol; Mg(OAc)<sub>2</sub>, magnesium acetate; Fmoc, 9-fluorenylmethoxycarbonyl; Boc, butyloxycarbonyl; PEI, polyethyleneimine; Z, *N*-benzyloxycarbonyl; dansyl, 5-dimethylamino-1-naphthalenesulfonyl; SDS, sodium dodecyl sulfate; PMSF, phenylmethanesulfonyl fluoride; DIPF, diisopropyl fluorophosphate; DMSO, dimethylsulfoxide; Kan, kanamycin; dlu, density light unit.

Table 1: Summary of Peptide-Based Substrates and Inhibitors

MG262	non-fluorescent				ZL <sub>3</sub> -B(OH) <sub>2</sub>
<b>2</b>	fluorescent	Y(3-NO <sub>2</sub> )RGIT-Abu-SGRQK(Abz)			
	non-fluorescent	YRGIT-Abu-SGRQK(Bz)			
<b>3</b>	fluorescent	dansyl-YRGIT-Abu			
<b>4</b>	fluorescent	dansyl-YRGIT-Abu-B(OH) <sub>2</sub>			
Y(3-NO <sub>2</sub> )	K(Abz)	K(Bz)	Abu	dansyl	
					

peptide bond hydrolysis (19, 23). Studies aimed at determining a consensus sequence for Lon cleavage have met with little success, as amino acid residues that are not adjacent to the scissile bond are important in recognition (9, 24–27). Furthermore, sequences important for recognition may or may not be substrates for peptide bond hydrolysis (24, 28).

Lon is unique, in that, although it is a serine protease, it is susceptible to both serine and cysteine protease inhibitors (29–32). Previously, none of the nucleotide- and peptide-based inhibitors identified were highly potent or specific (29–31). We recently reported the identification of the proteasome inhibitor MG262 (Table 1) as a potent ATP-dependent inhibitor of the proteolytic activity of *S. Typhimurium* Lon. In the current study, we employed steady-state enzyme kinetic techniques to investigate the mechanism by which MG262 inhibits the peptide hydrolysis activity of this protease. In addition, we synthesized a fluorescent peptidyl boronate inhibitor, **4** (Table 1), based upon the amino acid sequence of a product of peptide hydrolysis by the enzyme. We have demonstrated that both MG262 and **4** inhibit *S. Typhimurium* Lon peptide hydrolysis activity via the same competitive, two-step, time-dependent inhibition mechanism and with comparable potency. The dansyl moiety of **4** has also allowed us to monitor the ATP-dependent interaction of **4** with the active site serine of Lon.

## MATERIALS AND METHODS

**Materials.** All oligonucleotide primers were purchased from Integrated DNA Technologies, Inc. (Coralville, IA). All cloning reagents were purchased from Promega (Madison, WI), New England BioLabs, Inc. (Ipswich, MA), Invitrogen (Carlsbad, CA), and USB Corporation (Cleveland, OH). Fmoc-protected amino acids, Boc-2-Abz-OH, Fmoc-Lys(Aloc)-Wang resin, Fmoc-Abu-Wang resin, H-Thr(But)-2-Cl-Trt resin, and HBTU were purchased from Advanced ChemTech and NovaBiochem. MG262 was purchased from Biomol International, LP. Tris buffer, cell culture media, IPTG, chromatography media, DTT, Mg(OAc)<sub>2</sub>, trypsin, kanamycin, ATP, ADP, AMPPNP, dansyl chloride, DMSO, Tween 20, and all other materials were purchased from Fisher, Sigma, and Amresco (Solon, OH).

**Plasmid Construction.** A *S. Typhimurium* Lon mutant containing an alanine residue in place of the active site serine (S680A) was created using the QuikChange Site-Directed

Mutagenesis Kit (Stratagene) according to the manufacturer's instructions. The plasmid pHF020 (19) was used as a template, and oligonucleotides 5'-CCGAAAGACGGT-CCAGCCGCCGGTATCGCGATG-3' and 5'-CATCGCG-ATACCGGCGGCTGGACCGTCTTTCGG-3' were used as primers. The new plasmid, pHF031, was verified by DNA sequencing.

**Purification of Recombinant Lon.** Recombinant wild type and S680A *S. Typhimurium* Lon were overexpressed in BL21 (DE3) (Novagen), using the plasmids pHF020 and pHF031, respectively. Each was purified as previously published for *Escherichia coli* (*E. coli*) Lon (22) with the exception that 30 µg/mL Kan (Sigma) was used instead of 100 µg/mL Amp (Fisher). The concentration of Lon monomer was determined by Bradford assay, using BSA as a standard, and the purified protein stored at –80 °C.

**Peptide Synthesis.** Synthesis of **2**, **3**, and the nonfluorescent analogue of **2** (Table 1) were performed as previously described (22).

**Synthesis of 4.** The peptidyl boronate, **4** (Table 1), was synthesized by coupling (+)-pinanediol 1-amino-2-ethane-1-boronate hydrochloride to the peptidyl moiety as described below. The synthesis of (+)-pinanediol 1-amino-2-ethane-1-boronate hydrochloride was conducted via a three-step process using the procedure by Wityak et al. (33). Briefly, ethyl boronate was reacted with (+)-pinanediol in THF overnight to yield the (+)-pinanediol ester. The ester was treated with LDA in cyclohexane/THF (2:1, v/v) in the presence of CH<sub>2</sub>Cl<sub>2</sub> at –20 °C followed immediately by the addition of 1 M zinc chloride in THF at –20 °C. The resulting solution was warmed to room temperature and stirred overnight. The crude reaction mixture was purified by silica gel chromatography using hexane/ethyl acetate (95:5, v/v) and the desired reaction intermediate, (+)-pinanediol 1-chloro-2-ethane-1-boronate, characterized by <sup>1</sup>H and <sup>13</sup>C NMR (Supporting Information). The purified intermediate was treated with 0.5 M KHMDS (in toluene) at –20 °C in THF, followed by stirring at room temperature overnight to yield the TMS-protected amino boronate ester. The crude reaction mixture was concentrated to dryness and dissolved in hexane, followed by filtration. The filtrate was treated with 4 M HCl in dioxane at –10 °C to deprotect the amino group of the boronate ester. The boronate ester was recovered as the HCl salt through hexane precipitation. The final product,

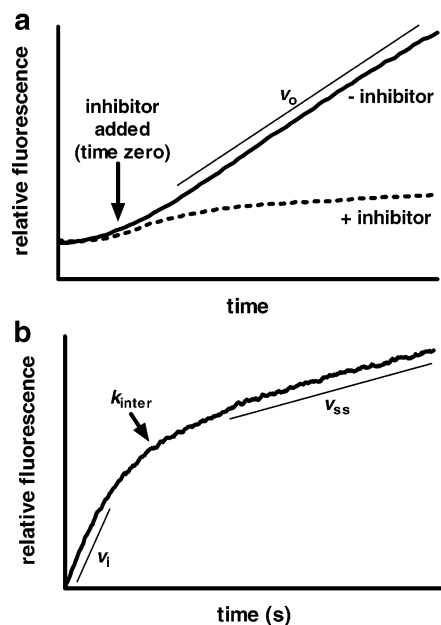


FIGURE 1: Experimental setup for measuring time-dependent inhibition of *S. Typhimurium* Lon peptide hydrolysis. (A) Representative time courses for *S. Typhimurium* Lon peptide hydrolysis in the absence (—) and presence (---) of a time-dependent inhibitor. In the absence of any inhibitor, time courses of Lon peptide hydrolysis display a lag prior to attaining steady-state turnover. When performing inhibition assays, the inhibitor was not added until steady-state turnover was reached and was considered time zero. The steady-state rate in the absence of inhibitor ( $v_o$ ) is indicated. (B) Representative time course for time-dependent inhibition of *S. Typhimurium* peptide hydrolysis. The initial ( $v_i$ ) and steady-state ( $v_{ss}$ ) rates are indicated as well as the rate constant for their interconversion,  $k_{inter}$ .

(+)-pinanediol 1-amino-2-ethane-1-boronate hydrochloride was characterized by  $^1\text{H}$  and  $^{13}\text{C}$  NMR (Supporting Information).

The peptide dansyl-Y(*t*-Bu)-R(Pbf)-GI-T(*t*-Bu)-OH was synthesized using Fmoc solid-phase synthesis techniques (34), starting with H-Thr(*t*-Bu)-2-Cl-Trt resin (Advanced ChemTech). The side chain protected peptide was released from the resin using acetic acid/TFE/ $\text{CH}_2\text{Cl}_2$  according to the manufacturer's instructions.

Finally, dansyl-Y(*t*-Bu)-R(Pbf)-GI-T(*t*-Bu)-OH was coupled to (+)-pinanediol 1-amino-2-ethane-1-boronate hydrochloride with EDC in THF. The amino acids were deprotected using 2.5% TIS/2.5% water/95% TFA. This was followed by removal of the pinanediol group with excess butyl boronate in water/diethyl ether (50:50, v/v). The desired peptidyl boronate (**4**) was purified by semipreparative reverse phase HPLC using a linear gradient from 20 to 25% acetonitrile/water/0.1% TFA over 20 min at 4 mL/min (retention time = 7.7 min). The predicted mass of the protonated form of **4** is 927.90 Da and was verified by ESI mass spectrometry ( $m/z$  = 927.43).

**Inhibition of Peptide Hydrolysis by *S. Typhimurium* Lon.** Steady-state velocity data were collected on a Fluoromax 3 spectrophotometer (Horiba Group) as previously described for *E. coli* Lon (22) with the following modifications. All reactions contained 50 mM Tris (pH 8.1), 10 mM Mg(OAc) $_2$ , 2 mM DTT, 30 nM *S. Typhimurium*, and varying concentrations of **2** (10% fluorescent/90% nonfluorescent). After equilibration at 37 °C for 1 min, the reaction was initiated by the addition of 1 mM ATP. Varying concentrations of

the inhibitor (MG262, **3**, or **4**) were added 50 s after the addition of ATP and was considered time zero for the inhibition reaction (Figure 1A). For classical inhibitors, the steady-state velocities were determined from the linear phase of the reaction time courses using KaleidaGraph (Synergy, Inc.). For time-dependent inhibitors, the steady-state velocities were determined by fitting the experimental time courses with eq 1 (35–37) using the nonlinear regression program Prism 4 (GraphPad Software, Inc.), with the exception of inhibition reactions containing <500 nM **4**. In these reactions, the steady-state velocities were determined from the final linear phase of the reaction time courses using KaleidaGraph (Synergy, Inc.).

$$P = v_{ss}t + \frac{v_i - v_{ss}}{k_{inter}}(1 - e^{-k_{inter}t}) \quad (1)$$

where  $P$  is the amount of peptide cleaved or fluorescent signal,  $v_{ss}$  is the final steady-state rate,  $t$  is time,  $v_i$  is the initial rate, and  $k_{inter}$  is the rate constant for the interconversion of  $v_{ss}$  and  $v_i$  (Figure 1B). All experiments were performed in triplicate. The use of eq 1 is allowed with tight-binding inhibitors when the following condition is satisfied:  $2[\text{Lon}] \leq [\text{inhibitor}] \leq K_i^{*app}$  (defined below) (36). All inhibitor concentrations evaluated satisfied this condition.

**Determination of the  $\text{IC}_{50}$  Value for **3** Inhibition of Peptide Hydrolysis by *S. Typhimurium* Lon.** The  $k_{obs}$  ( $v_{ss}/[\text{Lon}]$ ) data in the presence of 1 mM ATP, 300  $\mu\text{M}$  **2**, and varying concentrations of **3** were fit with eq 2 to obtain an  $\text{IC}_{50}$  value for the inhibitor (35).

$$\frac{k_{obs,i}}{k_{obs}} = \frac{1}{1 + \left(\frac{[I]}{\text{IC}_{50}}\right)^n} \quad (2)$$

where  $k_{obs,i}$  is the observed rate constant in the presence of **3**,  $k_{obs}$  is the observed rate constant in the absence of **3**,  $I$  is the inhibitor,  $\text{IC}_{50}$  is the  $[I]$  under which  $k_{obs,i}/k_{obs} = 0.5$ , and  $n$  is the Hill coefficient.

**Determination of the Mode for Peptidyl Boronate Inhibition of Peptide Hydrolysis by *S. Typhimurium* Lon.** The mode of inhibition was determined by fitting the  $k_{inter}$  data, at a single concentration of inhibitor and varying concentrations of **2**, with eq 3 for competitive time-dependent inhibition (35–37) using the nonlinear regression program Prism 4 (GraphPad Software, Inc.).

$$k_{inter} = \frac{k_{inter,max}}{1 + \frac{[S]}{K_m}} \quad (3)$$

where  $k_{inter}$  is as defined in eq 1,  $k_{inter,max}$  is the maximal value for  $k_{inter}$ ,  $S$  is the peptide substrate, and  $K_m$  is the Michaelis–Menton constant for the peptide substrate.

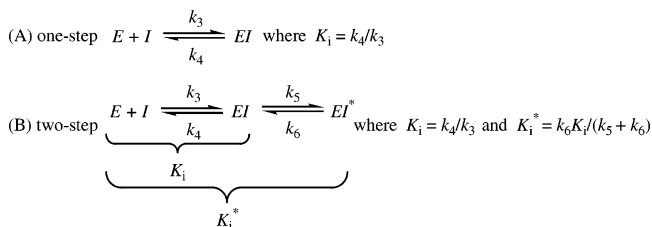
**Determination of the Mechanism for Peptidyl Boronate Inhibition of Peptide Hydrolysis by *S. Typhimurium* Lon.** The mechanism for inhibition was determined by fitting the  $v_i$  and  $v_{ss}$  data, at saturating **2** and varying concentrations of inhibitor, with eq 4 or 5 (35, 37) using the nonlinear regression program Prism 4 (GraphPad Software, Inc.). The use of eq 4 or 5 with tight-binding inhibitors is necessary to avoid errors due to significant changes in the concentration

Table 2: Summary of Parameters for Peptidyl Boronate Inhibition of *S. Typhimurium* Lon

	MG262	4
$k_3 (\times 10^5 \text{ M}^{-1} \text{ s}^{-1})$	$3.2 \pm 0.3$	$1.0 \pm 0.3$
$k_4 (\text{s}^{-1})$	$0.006 \pm 0.001$	$0.022 \pm 0.007$
$K_i (\text{nM})$	$19^a$	$216^a$
$k_5 (\text{s}^{-1})$	$0.0025 \pm 0.0006$	$0.0032 \pm 0.0003$
$k_6 (\text{s}^{-1})$	$0.0013 \pm 0.0001$	$0.00028 \pm 0.00002$
$K_i^* (\text{nM})$	$6.6^b$	$17^b$

<sup>a</sup> The value was determined using eq 8 as described in Materials and Methods. <sup>b</sup> The value was determined using eq 9 as described in Materials and Methods.

## Scheme 1: Time-Dependent Inhibition Mechanisms



of free enzyme during the experiment (35). The  $k_{\text{inter}}$  data, at saturating **2** and varying concentrations of inhibitor, were also fit with eq 6 (35–37) for two-step, time-dependent inhibition or eq 7 (35–37) for two-step, time-dependent inhibition in which  $K_i \gg K_i^*$  using the nonlinear regression program Prism 4 (GraphPad Software, Inc.).

$$\frac{v_i}{v_0} = 1 - \frac{([E] + [I] + K_i^{\text{app}}) - \sqrt{([E] + [I] + K_i^{\text{app}})^2 - 4[E][I]}}{2[E]} \quad (4)$$

$$\frac{v_{\text{ss}}}{v_0} = 1 - \frac{([E] + [I] + K_i^{*\text{app}}) - \sqrt{([E] + [I] + K_i^{*\text{app}})^2 - 4[E][I]}}{2[E]} \quad (5)$$

$$k_{\text{inter}} = k_6 + \left( \frac{k_5[I]}{K_i^{\text{app}} + [I]} \right) \quad (6)$$

$$k_{\text{inter}} = k_6 \left( 1 + \frac{[I]}{K_i^{*\text{app}}} \right) \quad (7)$$

where  $v_i$ ,  $v_{\text{ss}}$ , and  $k_{\text{inter}}$  are as defined in eq 1,  $I$  is the inhibitor,  $E$  is *S. Typhimurium* Lon monomer,  $v_0$  is the steady-state rate in the absence of inhibitor,  $K_i^{\text{app}}$  is the apparent dissociation constant for the initial Lon–inhibitor complex,  $K_i^{*\text{app}}$  is the apparent dissociation constant for the final Lon–inhibitor complex, and  $k_6$  and  $k_5$  are as defined in Scheme 1B.

**Determination of the Inhibition Constants for Peptidyl Boronate Inhibition of Peptide Hydrolysis by *S. Typhimurium* Lon.** Global nonlinear fitting of the averaged experimental time courses at saturating **2** and varying concentrations of inhibitor (6 total) was performed using DynaFit (BioKin Ltd.) (38). Differential equations were written for each species in

the two-step, time-dependent inhibition mechanism described in Scheme 1B as well as the uninhibited reaction and the reaction time courses fit directly. The values for  $K_i$  and  $K_i^*$  were then determined using the resultant rate constants in eq 8 and 9 (35–37), respectively, and are summarized in Table 2.

$$K_i = \frac{k_4}{k_3} \quad (8)$$

$$K_i^* = \frac{k_6 K_i}{k_5 + k_6} \quad (9)$$

where  $K_i$  is the dissociation constant for the initial Lon–inhibitor complex,  $K_i^*$  is the dissociation constant for the final Lon–inhibitor complex, and  $k_3$ ,  $k_4$ ,  $k_5$ , and  $k_6$  are as defined in Scheme 1B.

**Fluorescent Detection of the Interaction Between *S. Typhimurium* Lon and **4**.** Reactions containing 50 mM Tris (pH 8.1), 10 mM Mg(OAc)<sub>2</sub>, 2 mM DTT, 1  $\mu\text{M}$  **3** or **4**, and 1 mM of the indicated nucleotide were initiated by the addition of 100 nM–1  $\mu\text{M}$  *S. Typhimurium* Lon monomer. After incubation at 37 °C for 10 min, the emission spectrum (excitation polarizer = 0°, emission polarizer = 55°) from 500–600 nm was monitored using a Fluoromax 3 spectrophotometer (Horiba Group) after excitation at 335 nm. All reactions were performed in triplicate.

**Fluorescent Detection of the Reversibility of **4** Inhibition of *S. Typhimurium* Lon.** Reactions containing 50 mM Tris (pH 8.1), 10 mM Mg(OAc)<sub>2</sub>, 2 mM DTT, 1  $\mu\text{M}$  **4**, and 1 mM ATP or AMPPNP were equilibrated at 37 °C in the absence and presence of 100 nM *S. Typhimurium* Lon monomer prior to the addition of 0 or 10  $\mu\text{M}$  MG262 (in DMSO). After further equilibration at 37 °C for 3 h, the emission spectrum (excitation polarizer = 0°, emission polarizer = 55°) from 500–600 nm was monitored using a Fluoromax 3 spectrophotometer (Horiba Group) after excitation at 335 nm. All reactions were performed in triplicate.

**Determination of the Half-Life for Reversal of Inhibition.** The half-life for reversal of **4** inhibition was determined using eq 10 (35, 37).

$$t_{1/2} = \frac{\ln 2}{k_6} \quad (10)$$

where  $t_{1/2}$  is the half-life for reversal of inhibition, and  $k_6$  is as defined in Scheme 1B.

## RESULTS

**Lon Inhibition Assays.** We have previously demonstrated that MG262 (Table 1) is a potent time-dependent inhibitor of the peptide hydrolysis activity of *S. Typhimurium* Lon (19). Analysis of time-dependent kinetics requires monitoring the inhibition reaction using a continuous assay (36). We previously developed a continuous fluorescent peptide hydrolysis assay suitable for studying the inhibition of *S. Typhimurium* Lon by MG262 (39). Both **2** and the nonfluorescent analogue of **2** (Table 1) are hydrolyzed by *S. Typhimurium* Lon with similar kinetics (19). This allows us to use mixtures of the fluorescent and nonfluorescent peptides at high concentrations, thereby avoiding complications due to the inner filter effect.



Typically, time-dependent inhibition reactions are initiated by the addition of enzyme or substrate(s) (36). Because of the presence of an initial lag phase in the time course for peptide hydrolysis (19, 22), the inhibitor was not added to the reaction until after the completion of the lag phase (Figure 1A) in order to assess the effect of the inhibitor on the steady-state rate of peptide hydrolysis. As such, the inhibition time courses were defined by the addition of the inhibitor.

To accurately define both the initial and final phases of inhibition (Figure 1B), the time frame over which the inhibition reaction is monitored must be linear to avoid complications in our data analyses due to substrate depletion (36). To accomplish this, we used 10-fold less *S. Typhimurium* Lon monomer than that used in non-time-dependent peptide hydrolysis inhibition assays. In addition, saturating concentrations of ATP were included in all inhibition reactions to prevent the production of significant concentrations of ADP, which has been shown to inhibit the peptide hydrolysis activity of Lon (22, 40). Even under these reaction conditions, there are limitations in the range of inhibitor concentrations which could be evaluated. At high concentrations of the inhibitor, the lack of a significant fluorescent signal from peptide hydrolysis prevented an accurate determination of the initial rate. At low concentrations of the inhibitor, the final steady-state rate was not reached prior to the end of the linear phase. Therefore, the usable concentrations of inhibitors evaluated in the following studies were experimentally determined.

The  $K_d$  for formation of a Lon oligomer has yet to be determined. In order to avoid variations in the inhibition data because of differences in the oligomerization state of the enzyme, all inhibition reactions contained the same concentration of Lon monomer (30 nM).

*Dansyl-YRGIT-Abu-B(OH)<sub>2</sub> (4) as an Alternative Peptidyl Boronate Inhibitor.* MG262 is composed of a peptidyl moiety and a boronate moiety. Modifications to the peptidyl moiety have previously been used to improve the potency of peptidyl boronate inhibitors (41, 42). To further evaluate the structure–activity relationship between the amino acid sequence of the peptidyl moiety and efficacy of inhibition by peptidyl boronates, we synthesized **4** (Table 1). The peptidyl boronate, **4**, contains the amino acid sequence of a hydrolysis product of **2** and a boronic acid moiety in place of the C-terminal carboxyl group. In addition, the amino terminal of **4** was derivatized with a dansyl group to facilitate fluorescent detection of **4** interacting with Lon (see below). The peptidyl moiety of **4** (dansyl-YRGIT-Abu, **3**) has a much greater affinity for *S. Typhimurium* Lon than ZL<sub>3</sub>OH, as the  $IC_{50}$  value for inhibiting *S. Typhimurium* Lon peptide hydrolysis of **2** is  $89 \pm 9 \mu\text{M}$  (Figure 2), which is 8-fold greater than that previously obtained for ZL<sub>3</sub>OH ( $IC_{50} = 740 \pm 29 \mu\text{M}$ ) (19). As with ZL<sub>3</sub>OH, inhibition of the peptide hydrolysis activity of Lon by **3** was not time-dependent, indicating that binding was rapid (19).

*Time-Dependent Inhibition of S. Typhimurium Lon Peptide Hydrolysis by Peptidyl Boronate Inhibitors.* As with MG262, inhibition of *S. Typhimurium* Lon peptide hydrolysis by **4** is time-dependent (Figure 3) and requires the binding but not hydrolysis of ATP (Supporting Information). Most time-dependent enzyme inhibitors interact competitively with the analogous substrate (36); therefore, we evaluated whether the same mode of inhibition occurs with MG262 and **4**. This

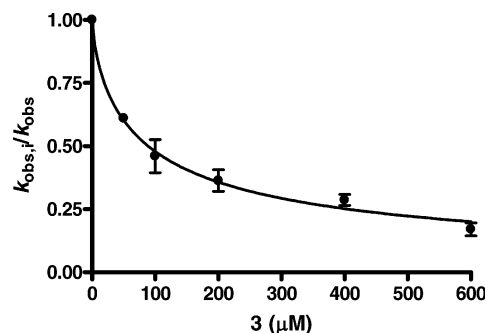


FIGURE 2: Inhibition of *S. Typhimurium* Lon peptide hydrolysis by **3**. Reactions containing 300 nM *S. Typhimurium* Lon were preincubated with 300  $\mu\text{M}$  **2** ( $K_m$  level) prior to the addition of 1 mM ATP. After 50 s, varying concentrations of **3** were added and peptide hydrolysis monitored over 10 min. All experiments were performed in triplicate and the  $k_{obs}$  values ( $v_{ss}/[\text{Lon}]$ ) determined as described in Materials and Methods. The averaged  $k_{obs}$  in the presence of **3**/ $k_{obs}$  in the absence of **3** ( $k_{obs,i}/k_{obs}$ ,  $\pm 1$  SD) were plotted against the corresponding inhibitor concentration. The  $IC_{50}$  ( $89 \pm 9 \mu\text{M}$ , with  $n = 0.72 \pm 0.08$ ) was determined by fitting the data to eq 2 as described in Materials and Methods.

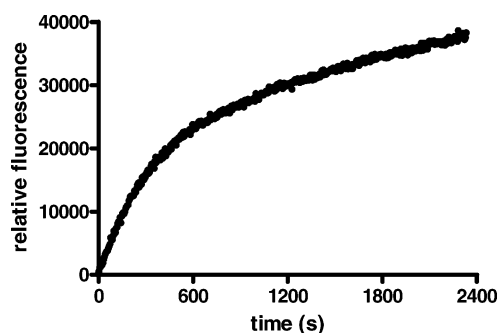


FIGURE 3: Time-dependent inhibition of *S. Typhimurium* Lon peptide hydrolysis by **4**. Representative time course for *S. Typhimurium* Lon (30 nM) degradation of 1 mM **2** in the presence of 1 mM ATP and 2  $\mu\text{M}$  **4**.

was done by determining the rate constant associated with the interconversion of the initial ( $v_i$ ) and final steady-state ( $v_{ss}$ ) rates,  $k_{inter}$ , at a fixed concentration of the inhibitor (MG262 or **4**) and varying concentrations of **2** (Figure 1B). The concentration of inhibitor was chosen such that both  $v_i$  and  $v_{ss}$  could be defined at all concentrations of **2** evaluated. As shown in Figure 4A and B, the value for  $k_{inter}$  decreases with increasing substrate concentration, indicating that both MG262 and **4** act as competitive inhibitors of the peptide substrate.

We previously proposed that MG262 inhibits via a two-step process (Scheme 1B) (19). Because the detection of the dependency of  $v_i$  and  $v_{ss}$  on the inhibitor concentration will provide support for this proposal (35–37), we determined the values for  $v_i$ ,  $v_{ss}$ , and  $k_{inter}$  for *S. Typhimurium* Lon hydrolysis of a fixed concentration of **2** and varying concentrations of inhibitor (MG262 and **4**). As shown in Figure 5A and B, both  $v_i$  and  $v_{ss}$  vary with increasing concentration of MG262 or **4**, supporting the existence of a two-step mechanism (Scheme 1B). Figure 6A also reveals that the  $k_{inter}$  data associated with MG262 inhibition of *S. Typhimurium* Lon varies hyperbolically with the concentration of MG262, further supporting a two-step inhibition mechanism (35–37). Interestingly, the  $k_{inter}$  data associated

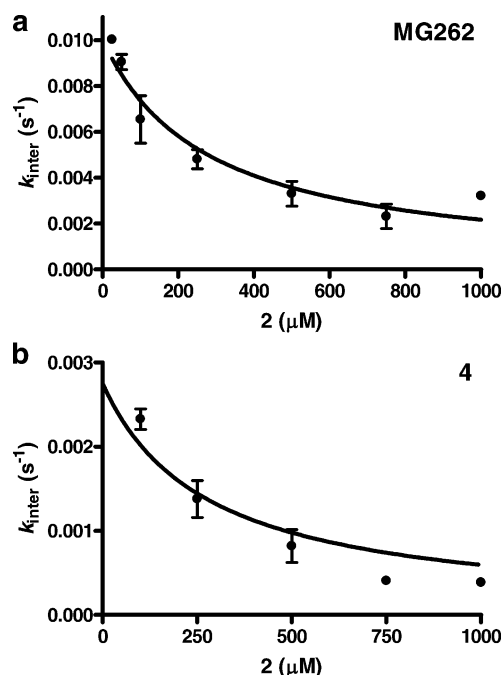


FIGURE 4: Peptidyl boronates are competitive inhibitors of *S. Typhimurium* Lon peptide hydrolysis. Reactions containing 30 nM *S. Typhimurium* Lon were preincubated with varying concentrations of **2** prior to the addition of 1 mM ATP. After 50 s, 300 nM MG262 (A) or 267 nM **4** (B) was added and peptide hydrolysis monitored over 40 min. All experiments were performed in triplicate and the  $k_{\text{inter}}$  values determined by fitting the time courses to eq 1 as described in Materials and Methods. The averaged  $k_{\text{inter}}$  ( $\pm 1$  SD) values were plotted against the corresponding peptide–substrate concentration. The solid line represents the best fit of the data with eq 3 for competitive time-dependent inhibition.

with **4** inhibition of *S. Typhimurium* Lon peptide hydrolysis varies linearly with the concentration of **4** (Figure 6B). A linear dependence of  $k_{\text{inter}}$  on the concentration of inhibitor is consistent with either a one-step inhibition mechanism (Scheme 1A) or a two-step inhibition mechanism in which the  $K_i \gg K_i^*$  (35–37). As both  $v_i$  and  $v_{ss}$  vary with the concentration of **4** (Figure 5B), indicating a two-step mechanism, it is plausible that the observed linear dependence represents the latter case. The magnitude of the reverse rate constant,  $k_6$  (Scheme 1B), was estimated by extrapolation of the data to zero inhibitor, which is the y-intercept shown in the insets of Figure 6A and B. The value appears to be greater than zero for both MG262 and **4**, suggesting that peptidyl boronate inhibition is reversible. Data at higher concentrations of **4** could not be obtained because of the lack of a significant fluorescent signal from peptide hydrolysis. Data at lower concentrations of **4** could not be obtained because  $v_{ss}$  was not obtained prior to the end of the linear phase of the uninhibited reaction.

To further evaluate the inhibition constants associated with peptidyl boronate inhibition of *S. Typhimurium* Lon, we globally fit the averaged experimental time courses at saturating **2** and varying concentrations of MG262 or **4** to a two-step time-dependent inhibition mechanism (Scheme 1B) using the nonlinear fitting program Dynafit (38) (Figure 7A and B). The resultant rate constants and the corresponding inhibition constants ( $K_i$  and  $K_i^*$ ) are summarized in Table 2. A nonzero value was obtained for the reverse rate constant  $k_6$  for both MG262 and **4**, further supporting that peptidyl boronate inhibition is reversible.

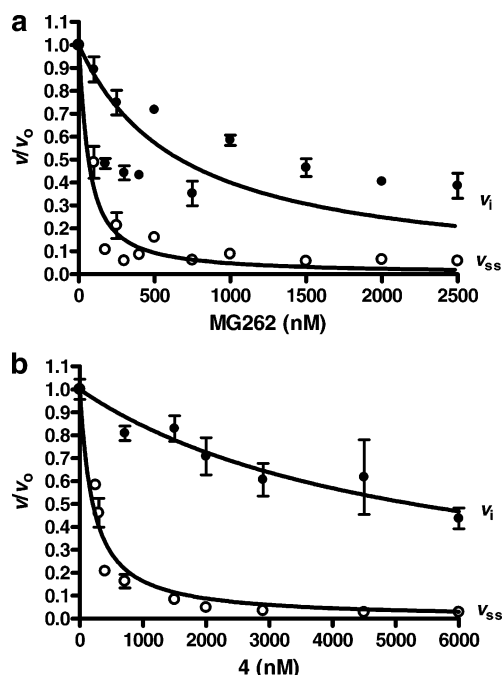


FIGURE 5: Initial and final steady-state rates for *S. Typhimurium* Lon peptide hydrolysis vary during inhibition by peptidyl boronates. Reactions containing 30 nM *S. Typhimurium* Lon were preincubated with 1 mM **2** prior to the addition of 1 mM ATP. After 50 s, varying concentrations of MG262 (A) or **4** (B) were added and peptide hydrolysis monitored over 40 min. All experiments were performed in triplicate and the  $v_i$  and  $v_{ss}$  values determined by fitting the time courses to eq 1 as described in Materials and Methods. The averaged  $v_i$  ( $\bullet$ ) or  $v_{ss}$  ( $\circ$ ) in the presence of inhibitor/ $v_{ss}$  in the absence of the inhibitor ( $v/v_0$ ,  $\pm 1$  SD) were plotted against the corresponding inhibitor concentrations. The solid lines represent the best fit of the data with eq 4 ( $v_i$ ) or eq 5 ( $v_{ss}$ ) for competitive inhibition.

*Characterization of the Interaction of S. Typhimurium Lon with 4 by Fluorescence Spectroscopy.* A fluorescent signal is often influenced by its environment (43). The dansyl moiety has been shown to undergo an increase in fluorescence upon binding to the more hydrophobic interior of a protein as well as a shift in the  $\lambda_{\text{max}}$  of the emission spectrum (43). To evaluate whether the fluorescent signal from **4** is altered upon binding to *S. Typhimurium* Lon, we monitored the emission spectrum ( $\lambda_{\text{excitation}} = 335$  nm) from 1  $\mu\text{M}$  **4** and 1 mM ATP in the presence and absence of 100 nM and 1  $\mu\text{M}$  *S. Typhimurium* Lon. In the presence of *S. Typhimurium* Lon, **4** undergoes a concentration-dependent increase in fluorescence and a shift in the  $\lambda_{\text{max}}$  of the emission spectrum from 555 to 545 nm (Figure 8A). The emission spectrum of control reactions containing buffer alone or buffer with *S. Typhimurium* Lon showed no fluorescence between 475 and 600 nm (data not shown). All emission spectra were collected under so-called magic angle conditions (excitation polarizer =  $0^\circ$ , emission polarizer =  $55^\circ$ ) to avoid interference due to scattered light.

In order to examine whether the active site serine is required for the interaction of **4** with *S. Typhimurium* Lon, we generated a *S. Typhimurium* Lon mutant in which the active site serine was replaced by an alanine residue (S680A *S. Typhimurium* Lon). This mutant displayed both intrinsic and peptide-stimulated ATP hydrolysis activity comparable to that of the wild type enzyme but was unable to catalyze peptide bond hydrolysis (Supporting Information). This property is also observed in the analogous *Escherichia coli*

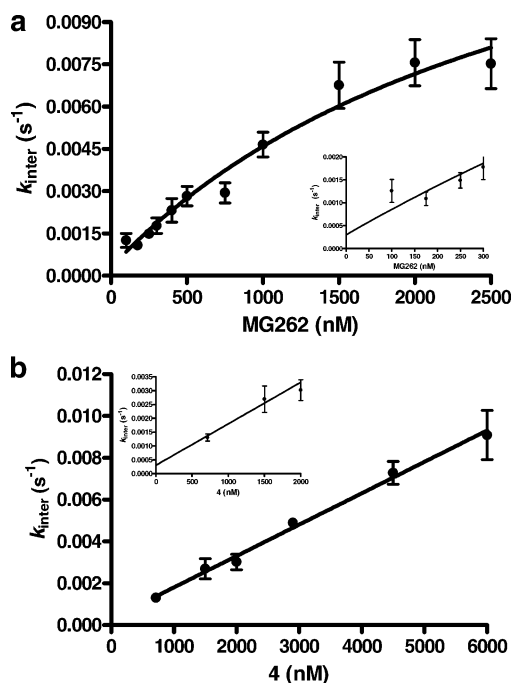


FIGURE 6: Peptidyl boronates inhibit *S. Typhimurium* Lon peptide hydrolysis via a two-step mechanism. Reactions containing 30 nM *S. Typhimurium* Lon were preincubated with 1 mM **2** prior to the addition of 1 mM ATP. After 50 s, varying concentrations of MG262 (A) or **4** (B) were added and peptide hydrolysis monitored over 40 min. All experiments were performed in triplicate and the  $k_{\text{inter}}$  values determined by fitting the time courses to eq 1 as described in Materials and Methods. The averaged  $k_{\text{inter}}$  ( $\pm 1$  SD) data were plotted against the corresponding inhibitor concentration. The solid lines represent the best fit of the data with eq 6 (A) or eq 7 (B) for competitive inhibition.

Lon mutant (9). We monitored the emission spectrum from 1  $\mu\text{M}$  **4** and 1 mM ATP in the absence and presence of 100 nM wild type or S680A *S. Typhimurium* Lon (Figure 8B). No increase in fluorescence was observed, indicating that the active site serine is required for interaction of **4** with Lon.

Inhibition of *S. Typhimurium* Lon by **4** requires the binding but not hydrolysis of ATP (Supporting Information). Therefore, we predict that the altered fluorescent signal from **4** interacting with *S. Typhimurium* Lon will still be observed in the presence of AMPPNP, a nonhydrolyzable analogue of ATP, but not in the absence of nucleotide. We monitored the emission spectrum from 1  $\mu\text{M}$  **4** and 1  $\mu\text{M}$  wild type *S. Typhimurium* Lon in the presence of 1 mM ATP, 1 mM AMPPNP, or no nucleotide. Indeed, the increase in fluorescence and shift of the  $\lambda_{\text{max}}$  to 545 nm was observed only in the presence of 1 mM ATP or AMPPNP (Figure 8C). Interestingly, we did not observe an increase in fluorescence in the presence of 1 mM ADP, implying that although hydrolysis of ATP is not necessary for inhibition, the presence of the gamma phosphate is required.

The value of the reverse rate constant,  $k_6$ , is nonzero for both MG262 and **4** (Table 2), indicating that inhibition of *S. Typhimurium* Lon by peptidyl boronates is reversible. To further evaluate the reversibility of **4** inhibition of *S. Typhimurium* Lon, we preincubated 100 nM *S. Typhimurium* Lon with 1  $\mu\text{M}$  **4** and 1 mM ATP or AMPPNP for 30 min prior to the addition of 10  $\mu\text{M}$  MG262. If inhibition by **4** is reversible, we predict that after four half-lives for reversal

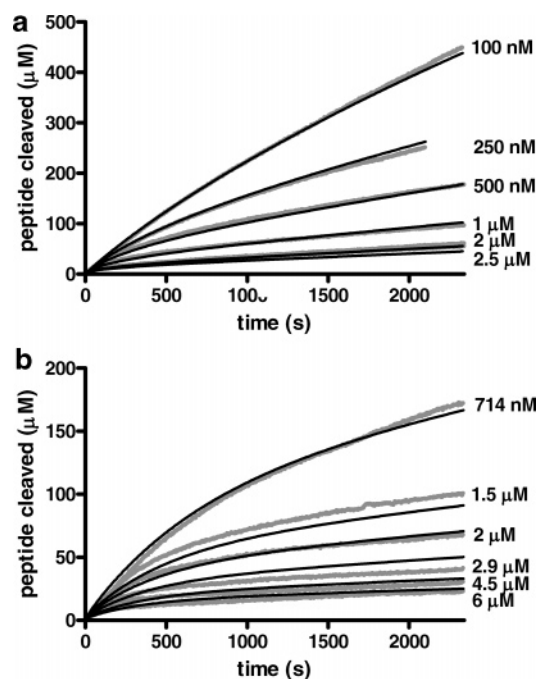


FIGURE 7: Global nonlinear fitting of the inhibition of *S. Typhimurium* Lon peptide hydrolysis by peptidyl boronates. The graylines represent the averaged experimental time courses at saturating **2** and varying concentrations of MG262 (A) or **4** (B). The black lines represent the best fit resulting from global nonlinear fitting of the experimental time courses to a two-step, time-dependent inhibition mechanism (Scheme 1B) using DynaFit (BioKin Ltd.).

of inhibition ( $\sim 3$  h), the excess MG262 will replace **4** in the active site of *S. Typhimurium* Lon, leading to a loss of the altered fluorescent signal associated with *S. Typhimurium* Lon interaction with **4**. As shown in Figure 9, in the presence of ATP and MG262, the increase in fluorescence associated with *S. Typhimurium* Lon interaction with **4** is lost. As a control, the experiment was also performed in the absence of MG262 (DMSO only), and the increase in fluorescence was maintained. Similar results were obtained with AMPPNP (data not shown).

## DISCUSSION

Lon, also known as the protease La, belongs to the AAA<sup>+</sup> superfamily (ATPases Associated with different cellular Activities) along with other ATP-dependent proteases, such as ClpXP, HslUV, and the proteasome (4, 5). Despite the presence of a Ser-Lys dyad in the proteolytic active site, Lon is relatively unreactive toward small serine protease inhibitors such as PMSF or DIFP (20, 29–31). In the presence of ATP or the nonhydrolyzable analogue AMPPNP, the peptide hydrolysis activity of *S. Typhimurium* Lon is readily inhibited by the peptidyl boronate, MG262 ( $\text{IC}_{50} = 122 \pm 9$  nM) (19). These results suggest that a residue within the proteolytic active site may require allosteric activation induced by ATP binding. As *S. Typhimurium* Lon activity has been shown to be important for virulence in a study model for typhoid fever in humans (2), an understanding of the mechanism by which MG262 inhibits this enzyme will provide insight that will benefit the design of novel therapeutic agents to combat salmonellosis.

In this study, we employed steady-state enzyme kinetic techniques to investigate the mechanism by which MG262



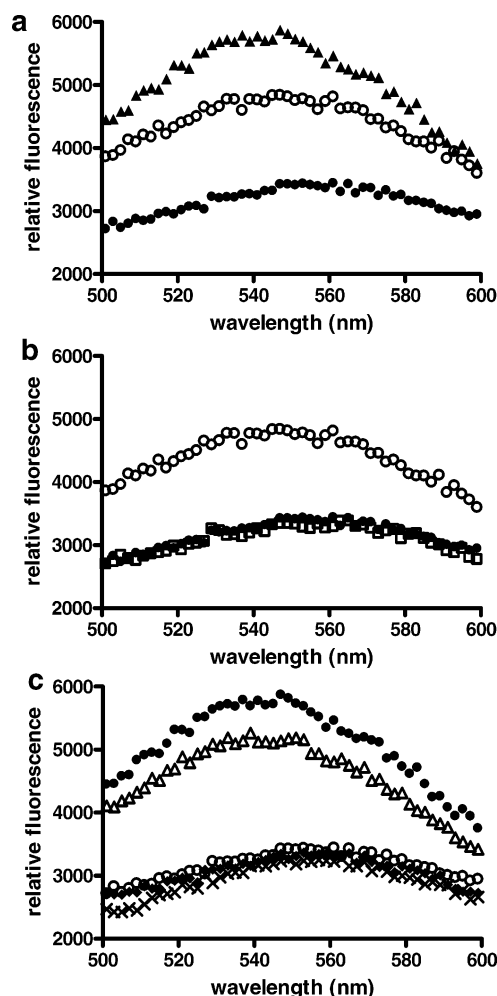


FIGURE 8: Fluorescent detection of the interaction between *S. Typhimurium* Lon and **4**. Representative emission spectra ( $\lambda_{\text{excitation}} = 335$  nm) from reactions containing  $1 \mu\text{M}$  **4**,  $1$  mM of the indicated nucleotide, and varying concentrations of *S. Typhimurium* Lon were equilibrated at  $37^\circ\text{C}$  for  $10$  min. All reactions were performed in triplicate. (A) Emission spectra in the presence of  $0$  nM ( $\bullet$ ),  $100$  nM ( $\circ$ ), or  $1 \mu\text{M}$  ( $\blacktriangle$ ) *S. Typhimurium* Lon and  $1$  mM ATP. (B) Emission spectra in the absence ( $\bullet$ ) and presence of  $100$  nM wild type ( $\circ$ ) or S680A ( $\square$ ) *S. Typhimurium* Lon and  $1$  mM ATP. (C) Emission spectra in the absence of *S. Typhimurium* Lon ( $\circ$ ) or in the presence of  $1 \mu\text{M}$  *S. Typhimurium* Lon and  $1$  mM ATP ( $\bullet$ ),  $1$  mM AMPPNP ( $\Delta$ ),  $1$  mM ADP ( $\blacklozenge$ ), or no nucleotide ( $\times$ ).

inhibits the peptide hydrolysis activity of *S. Typhimurium* Lon. In addition, we synthesized a fluorescent peptidyl boronate inhibitor, **4** (Table 1), based upon the amino acid sequence of a product of peptide hydrolysis by the enzyme. We have demonstrated that **4** inhibits *S. Typhimurium* Lon peptide hydrolysis activity via the same two-step, time-dependent mechanism and with comparable potency, as MG262 (Table 2). The fluorescent dansyl moiety of **4** has also allowed us to monitor the targeted interaction of **4** with the active site serine of the enzyme.

Analysis of the time courses for time-dependent inhibition of *S. Typhimurium* Lon peptide hydrolysis by MG262 and **4** has allowed us to construct a minimal kinetic model for their mechanism of inhibition. Examination of the dependence of the initial ( $v_i$ ) and final steady-state ( $v_{ss}$ ) rates for peptide hydrolysis in the presence of MG262 or **4** reveal that both are inversely dependent on the concentration of inhibitor (Figure 5A and B). This relationship qualitatively

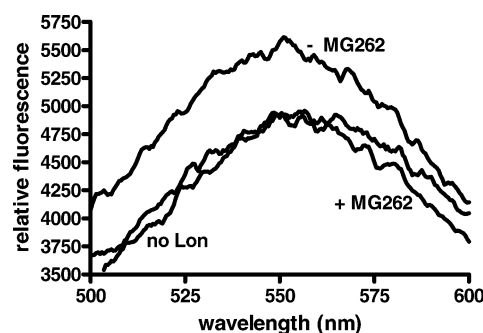


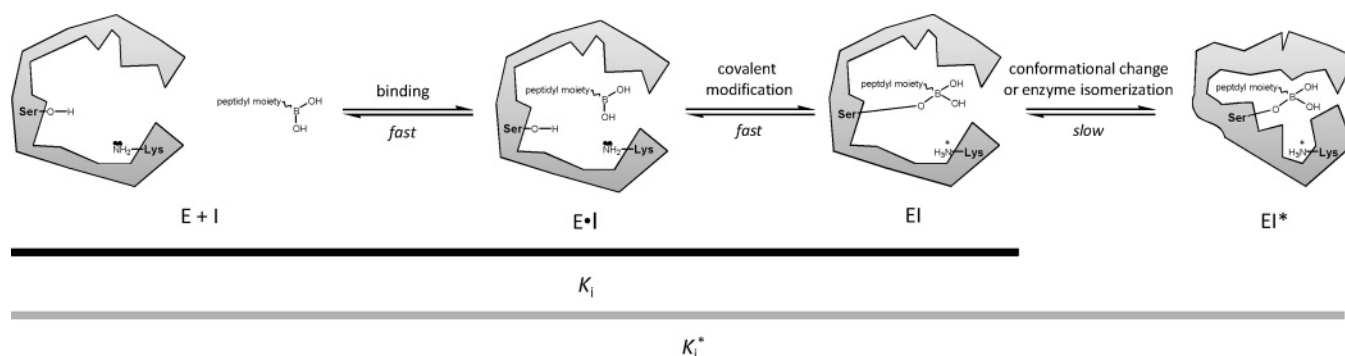
FIGURE 9: Compound **4** is a reversible inhibitor of *S. Typhimurium* Lon. Reactions containing  $0$  or  $100$  nM *S. Typhimurium* Lon and  $1$  mM ATP were preincubated with  $1 \mu\text{M}$  **4** for  $30$  min at  $37^\circ\text{C}$  prior to the addition of  $0$  or  $10 \mu\text{M}$  MG262 (in DMSO). Representative emission spectra ( $\lambda_{\text{excitation}} = 335$  nm) of reactions after further equilibration at  $37^\circ\text{C}$  for  $3$  h are shown. All reactions were performed in triplicate. The generation of a large concentration of ADP, which does not support complex formation (Figure 8C), resulted in a decreased signal compared to that observed in Figure 8A.

confirms a two-step time-dependent inhibition mechanism (Scheme 1B) (35–37). In order to quantitatively define the inhibition constants associated with peptidyl boronate inhibition of *S. Typhimurium* Lon, we utilized the nonlinear fitting program Dynafit to globally fit the peptide hydrolysis time courses to a two-step inhibition mechanism (Figure 7A and B; Table 2). A two-step mechanism should also result in a hyperbolic dependence of  $k_{\text{inter}}$  (the rate constant for the interconversion of  $v_i$  and  $v_{ss}$ ) on the concentration of inhibitor (35–37). This dependence is detected with inhibition by MG262 (Figure 6A), which has only a 3-fold difference in  $K_i$  and  $K_i^*$  (Table 2). The observation of a linear dependence of  $k_{\text{inter}}$  on the concentration of **4**, despite being a two-step mechanism, is supported by the much larger 10-fold difference in  $K_i$  and  $K_i^*$  (Table 2). To detect the hyperbolic dependence, the inhibitor would need to be varied over a much larger range, which was not possible because of the technical limitations of the assay.

The two-step, time-dependent inhibition mechanism has been observed in peptidyl boronate inhibition of classical serine protease inhibitors (44). The first step is rapid and proposed to be the binding of the inhibitor and the formation of a tetrahedral adduct. This is followed by a second slow step in which the enzyme undergoes a reversible rearrangement of the active site residues, thereby strengthening the interaction between the enzyme and inhibitor (44). The mode of inhibition for both MG262 and **4** is competitive with respect to the peptide substrate (Figure 4A and B), and the presence of the peptidyl moiety is required for inhibition by MG262 (19). Furthermore, fluorescence spectroscopic studies reveal that the presence of the active site serine of *S. Typhimurium* Lon is required for interaction with **4** (Figure 8B). Taken together, these results suggest that the binding interaction between the peptidyl moiety of MG262 and **4** serves to direct the boronate moiety to the proteolytic site of Lon. The requirement for the active site serine suggests that the enzyme may form a covalent adduct with this residue. Attempts to detect the covalent adduct by both fluorescence spectroscopy and SDS–PAGE were unsuccessful (data not shown). The difficulty in detecting the tetrahedral intermediate is presumed to be the high  $pK_a$  ( $>10$ ) of the trivalent boronate, a weak Lewis acid, which would



Scheme 2



require a strong base to stabilize the tetrahedral adduct (45). Confirmation of a covalent adduct will therefore require X-ray crystallographic studies with the peptidyl boronate bound to the active site.

The  $K_i$  value for the inhibitor represents the affinity of the inhibitor for the initial EI complex (Scheme 1B). If the first step represented simple binding of the peptidyl boronate to *S. Typhimurium* Lon, we would expect the  $K_i$  values of MG262 and **4** to be comparable to that of their cognate peptidyl moieties (ZL<sub>3</sub>OH and **3**, respectively). Estimation of  $K_i$  from the IC<sub>50</sub> values, as previously described (19), results in  $K_i$  values of 355 and 43  $\mu$ M for ZL<sub>3</sub>OH and **3**, respectively. These are substantially higher than the true values (Table 2) by a factor of  $10^2$ – $10^4$ . It is highly unlikely that substitution of the carboxyl group by the boronate group would lead to this large increase in affinity; thus, the first phase of inhibition must involve at least two rapid steps. We propose that like that of the classical serine proteases (44), the first step describes both the binding of the inhibitor and the formation of the putative covalent adduct. If the first phase represented the binding of the inhibitor followed by a noncovalent interaction such as a conformational change, we would expect to observe an increase in fluorescence of **4** in the absence of the active site serine. However, no increase in fluorescence is observed, even in the presence of ATP (Figure 8B).

To account for the slow step, which results in the observation of time-dependent inhibition, we propose a conformational change or isomerization event such as that observed with classical serine proteases (44), which results in an enhanced interaction between the peptidyl boronate and Lon. The values for  $k_5$ , which correspond to conversion from EI to EI\*, are comparable for both MG262 and **4** (Table 2), implying that the rearrangement of the proteolytic active site to enhance interaction between Lon and the inhibitor is not dependent on the inhibitor. However, the values for  $k_6$ , which correspond to the conversion of EI\* back to EI, are 5-fold slower with **4** (Table 2). This suggests that **4**, whose peptidyl moiety mimics the product of peptide hydrolysis by *S. Typhimurium* Lon, forms a more stable interaction with the enzyme. Further modification of the peptidyl moiety in future inhibitors may increase their overall affinity ( $K_i^*$ ). The global fitting analysis resulted in a nonzero value for  $k_6$  (Table 2), for both MG262 and **4**, which implies that the inhibition is reversible. This is confirmed by the loss of the increased fluorescent signal resulting from the interaction of **4** with *S. Typhimurium* Lon when excess MG262 is introduced into the reaction (Figure 9). The excess MG262

sequesters the free *S. Typhimurium* Lon upon dissociation of **4** from the active site.

Our previous studies highlighted a unique feature of MG262 inhibition of *S. Typhimurium* Lon peptide hydrolysis activity, that is, it requires the binding of ATP (19). Typically, ATP is not required for the inhibition of serine or threonine proteases by peptidyl boronates, even those that are physiologically ATP-dependent (44, 46, 47). We have demonstrated that **4** also requires the binding of ATP to inhibit peptide hydrolysis by *S. Typhimurium* Lon (Supporting Information). The dansyl moiety of **4** has allowed us to probe its interaction with the enzyme by fluorescence spectroscopy. The interaction of **4** with *S. Typhimurium* Lon is observed in the presence of ATP and AMPPNP but not in the presence of ADP or in the absence of any nucleotide (Figure 8C). The presence of only the adenine base or the hydrolysis of ATP is not sufficient to support inhibition by **4**; the observed inhibition also requires the presence of the gamma phosphate. These results suggest that a residue within the proteolytic active site of Lon may require allosteric activation induced by ATP binding. Previous studies have confirmed the existence of a conformational change in *E. coli* Lon upon binding of ATP, AMPPNP, and ADP (23). However, this work provides evidence that the conformational change detected in the presence of ATP and AMPPNP is different from that in the presence of ADP. Understanding the role of ATP in facilitating the inhibition of *S. Typhimurium* Lon peptide hydrolysis will require further investigation and will provide insight useful in the design of future Lon inhibitors.

In this study, we have demonstrated that **4** inhibits *S. Typhimurium* Lon peptide hydrolysis activity via the same two-step, time-dependent mechanism, and with comparable potency, as MG262 (Table 2). The overall mechanism for inhibition involves three steps (Scheme 2). First, the peptidyl boronate binds to *S. Typhimurium* Lon to form an initial complex (E•I). This is followed by rapid nucleophilic attack on the boronate by the active site serine to form a tetrahedral intermediate (EI). Finally, *S. Typhimurium* Lon undergoes an isomerization or conformational change, which enhances the interaction between the peptidyl boronate and Lon (EI\*). The first two steps occur rapidly and are represented by the inhibitor dissociation constant  $K_i$  (Table 2). Although ATP binding is required to detect the EI\* complex, it is unclear whether the first, second, or both steps are dependent on ATP binding. After the slow formation of EI\* complex, the overall inhibition constant, representing all three steps, is given by  $K_i^*$  (Table 2). Further studies are currently underway

to determine whether this unique ATP-dependent inhibition mechanism also occurs in the human homologue.

The peptidyl boronate **4** will be useful as a mechanistic probe in future studies of Lon and other serine and threonine proteases because it contains a fluorescent dansyl moiety with which the interaction of the enzyme and peptidyl boronate in the absence of a peptide or protein substrate can be monitored. Previous studies have demonstrated that peptidyl boronates are able to diffuse into the cell and even the mitochondria (42, 48). In fact, the proteasome inhibitor bortezomib, a peptidyl boronate currently used in the treatment of multiple myeloma, causes mitochondrial damage by an unknown mechanism (48, 49). As modifications to the peptidyl moiety have previously been used to improve the potency of peptidyl boronate inhibitors (41, 42), this approach may be useful in developing peptidyl boronates that discriminate between various proteases. Thus, **4** will serve as a lead compound in the development of enzyme-specific peptidyl boronates that will minimize cross-reactivity with other proteases and allow each protease to be studied independently *in vivo*.

## ACKNOWLEDGMENT

We thank Xuemei Zhang, Jason Hudak, Edward Motea, and Jessica Ward for aid in NMR and mass spectral analysis. We also thank Donald S. Matteson for suggestions regarding the synthesis of peptidyl boronates. Finally, we greatly appreciate the help from Jennifer Fishovitz, Diana Vineyard, Jessica Ward, and Tony Berdis in preparing this manuscript.

## SUPPORTING INFORMATION AVAILABLE

Details of the ATP dependence of inhibition, steady-state kinetic characterization of the S680A *S. Typhimurium* Lon mutant, and NMR data. This material is available free of charge via the Internet at <http://pubs.acs.org>.

## REFERENCES

- Robertson, G. T., Kovach, M. E., Allen, C. A., Ficht, T. A., and Roop, R. M., II. (2000) The *Brucella abortus* Lon functions as a generalized stress response protease and is required for wild-type virulence in BALB/c mice, *Mol. Microbiol.* **35**, 577–588.
- Takaya, A., Suzuki, M., Matsui, H., Tomoyasu, T., Sashinami, H., Nakane, A., and Yamamoto, T. (2003) Lon, a stress-induced ATP-dependent protease, is critically important for systemic *Salmonella enterica* serovar typhimurium infection of mice, *Infect. Immun.* **71**, 690–696.
- Matsui, H., Suzuki, M., Isshiki, Y., Kodama, C., Eguchi, M., Kikuchi, Y., Motokawa, K., Takaya, A., Tomoyasu, T., and Yamamoto, T. (2003) Oral immunization with ATP-dependent protease-deficient mutants protects mice against subsequent oral challenge with virulent *Salmonella enterica* serovar typhimurium, *Infect. Immun.* **71**, 30–39.
- Dougan, D. A., Mogk, A., Zeth, K., Turgay, K., and Bukau, B. (2002) AAA+ proteins and substrate recognition, it all depends on their partner in crime, *FEBS Lett.* **529**, 6–10.
- Patel, S., and Latterich, M. (1998) The AAA team: related ATPases with diverse functions, *Trends Cell Biol.* **8**, 65–71.
- Charette, M. F., Henderson, G. W., Doane, L. L., and Markovitz, A. (1984) DNA-stimulated ATPase activity on the lon (CapR) protein, *J. Bacteriol.* **158**, 195–201.
- Chung, C. H., and Goldberg, A. L. (1981) The product of the lon (capR) gene in *Escherichia coli* is the ATP-dependent protease, protease La, *Proc. Natl. Acad. Sci. U.S.A.* **78**, 4931–4935.
- Goff, S. A., and Goldberg, A. L. (1985) Production of abnormal proteins in *E. coli* stimulates transcription of lon and other heat shock genes, *Cell* **41**, 587–595.
- Goldberg, A. L., Moerschell, R. P., Chung, C. H., and Maurizi, M. R. (1994) ATP-dependent protease La (lon) from *Escherichia coli*, *Methods Enzymol.* **244**, 350–375.
- Goldberg, A. L., and Waxman, L. (1985) The role of ATP hydrolysis in the breakdown of proteins and peptides by protease La from *Escherichia coli*, *J. Biol. Chem.* **260**, 12029–12034.
- Gottesman, S. (1996) Proteases and their targets in *Escherichia coli*, *Annu. Rev. Genet.* **30**, 465–506.
- Gottesman, S., Gottesman, M., Shaw, J. E., and Pearson, M. L. (1981) Protein degradation in *E. coli*: the lon mutation and bacteriophage lambda N and cII protein stability, *Cell* **24**, 225–233.
- Gottesman, S., and Maurizi, M. R. (1992) Regulation by proteolysis: energy-dependent proteases and their targets, *Microbiol. Rev.* **56**, 592–621.
- Maurizi, M. R. (1992) Proteases and protein degradation in *Escherichia coli*, *Experientia* **48**, 178–201.
- Schoemaker, J. M., Gayda, R. C., and Markovitz, A. (1984) Regulation of cell division in *Escherichia coli*: SOS induction and cellular location of the sulA protein, a key to lon-associated filamentation and death, *J. Bacteriol.* **158**, 551–561.
- Suzuki, C. K., Kutejova, E., and Suda, K. (1995) Analysis and purification of ATP-dependent mitochondrial lon protease of *Saccharomyces cerevisiae*, *Methods Enzymol.* **260**, 486–494.
- Wang, N., Maurizi, M. R., Emmert-Buck, L., and Gottesman, M. M. (1994) Synthesis, processing, and localization of human Lon protease, *J. Biol. Chem.* **269**, 29308–29313.
- Huang, X., and Miller, W. (1991) A time-efficient, linear-space local similarity algorithm, *Advances in Applied Mathematics* **12**, 337–357.
- Frase, H., Hudak, J., and Lee, I. (2006) Identification of the proteasome inhibitor MG262 as a potent ATP-dependent inhibitor of the *Salmonella enterica* serovar Typhimurium Lon protease, *Biochemistry* **45**, 8264–8274.
- Botos, I., Melnikov, E. E., Cherry, S., Khalatova, A. G., Rasulova, F. S., Tropea, J. E., Maurizi, M. R., Rotanova, T. V., Gustchina, A., and Wlodawer, A. (2004) Crystal structure of the AAA+ alpha domain of *E. coli* Lon protease at 1.9 Å resolution, *J. Struct. Biol.* **146**, 113–122.
- Lowe, J., Stock, D., Jap, B., Zwickl, P., Baumeister, W., and Huber, R. (1995) Crystal structure of the 20S proteasome from the archaeon *T. acidophilum* at 3.4 Å resolution, *Science* **268**, 533–539.
- Thomas-Wohlever, J., and Lee, I. (2002) Kinetic characterization of the peptidase activity of *Escherichia coli* Lon reveals the mechanistic similarities in ATP-dependent hydrolysis of peptide and protein substrates, *Biochemistry* **41**, 9418–9425.
- Patterson, J., Vineyard, D., Thomas-Wohlever, J., Behshad, R., Burke, M., and Lee, I. (2004) Correlation of an adenine-specific conformational change with the ATP-dependent peptidase activity of *Escherichia coli* Lon, *Biochemistry* **43**, 7432–7442.
- Gonzalez, M., Frank, E. G., Levine, A. S., and Woodgate, R. (1998) Lon-mediated proteolysis of the *Escherichia coli* UmuD mutagenesis protein: in vitro degradation and identification of residues required for proteolysis, *Genes Dev.* **12**, 3889–3899.
- Maurizi, M. R. (1987) Degradation in vitro of bacteriophage lambda N protein by Lon protease from *Escherichia coli*, *J. Biol. Chem.* **262**, 2696–2703.
- Van Melder, L., Thi, M. H., Lecchi, P., Gottesman, S., Couturier, M., and Maurizi, M. R. (1996) ATP-dependent degradation of CcdA by Lon protease. Effects of secondary structure and heterologous subunit interactions, *J. Biol. Chem.* **271**, 27730–27738.
- Nishii, W., Maruyama, T., Matsuoka, R., Muramatsu, T., and Takahashi, K. (2002) The unique sites in SulA protein preferentially cleaved by ATP-dependent Lon protease from *Escherichia coli*, *Eur. J. Biochem.* **269**, 451–457.
- Higashitani, A., Ishii, Y., Kato, Y., and Koriuchi, K. (1997) Functional dissection of a cell-division inhibitor, SulA, of *Escherichia coli* and its negative regulation by Lon, *Mol. Gen. Genet.* **254**, 351–357.
- Bota, D. A., and Davies, K. J. (2002) Lon protease preferentially degrades oxidized mitochondrial aconitase by an ATP-stimulated mechanism, *Nat. Cell Biol.* **4**, 674–680.
- Waxman, L., and Goldberg, A. L. (1982) Protease La from *Escherichia coli* hydrolyzes ATP and proteins in a linked fashion, *Proc. Natl. Acad. Sci. U.S.A.* **79**, 4883–4887.

31. Waxman, L., and Goldberg, A. L. (1985) Protease La, the lon gene product, cleaves specific fluorogenic peptides in an ATP-dependent reaction, *J. Biol. Chem.* 260, 12022–12028.
32. Kisselev, A. F., and Goldberg, A. L. (2001) Proteasome inhibitors: from research tools to drug candidates, *Chem. Biol.* 8, 739–758.
33. Wityak, J., Earl, R. A., Abelman, M. M., Bethel, Y. B., Fisher, B. N., Kauffman, G. S., Kettner, C. A., Ma, P., Mcmillan, J. L., Mersinger, L. J., Pesti, J., Pierce, M. E., Rankin, F. W., Chorvat, R. J., and Confalone, P. N. (1995) Synthesis of thrombin inhibitor Dup-714, *J. Org. Chem.* 60, 3717–3722.
34. Wellings, D. A., and Atherton, E. (1997) Standard Fmoc protocols, *Methods Enzymol.* 289, 44–67.
35. Copeland, R. A. (2000) *Enzymes: A Practical Introduction to Structure, Mechanism, and Data Analysis*, 2nd ed., John Wiley & Sons, Inc., New York.
36. Morrison, J. F., and Walsh, C. T. (1988) The behavior and significance of slow-binding enzyme inhibitors, *Adv. Enzymol. Relat. Areas Mol. Biol.* 61, 201–301.
37. Copeland, R. A. (2005) *Evaluation of Enzyme Inhibitors in Drug Discovery: A Guide for Medicinal Chemists and Pharmacologists*, John Wiley & Sons, Inc., Hoboken, NJ.
38. Kuzmic, P. (1996) Program DYNAFIT for the analysis of enzyme kinetic data: application to HIV proteinase, *Anal. Biochem.* 237, 260–273.
39. Lee, I., and Berdis, A. J. (2001) Adenosine triphosphate-dependent degradation of a fluorescent lambda N substrate mimic by Lon protease, *Anal. Biochem.* 291, 74–83.
40. Menon, A. S., and Goldberg, A. L. (1987) Protein substrates activate the ATP-dependent protease La by promoting nucleotide binding and release of bound ADP, *J. Biol. Chem.* 262, 14929–14934.
41. Adams, J., Behnke, M., Chen, S., Cruickshank, A. A., Dick, L. R., Grenier, L., Klunder, J. M., Ma, Y. T., Plamondon, L., and Stein, R. L. (1998) Potent and selective inhibitors of the proteasome: dipeptidyl boronic acids, *Bioorg. Med. Chem. Lett.* 8, 333–338.
42. Adams, J., Palombella, V. J., Sausville, E. A., Johnson, J., Destree, A., Lazarus, D. D., Maas, J., Pien, C. S., Prakash, S., and Elliott, P. J. (1999) Proteasome inhibitors: a novel class of potent and effective antitumor agents, *Cancer Res.* 59, 2615–2622.
43. Lakowicz, J. R. (1999) *Principles of Fluorescence Spectroscopy*, 2nd ed., Plenum Press, New York.
44. Kettner, C. A., and Shenvi, A. B. (1984) Inhibition of the serine proteases leukocyte elastase, pancreatic elastase, cathepsin G, and chymotrypsin by peptide boronic acids, *J. Biol. Chem.* 259, 15106–15114.
45. Hall, D. G. (2005) *Boronic Acids: Preparation and Applications in Organic Synthesis and Medicine*, 1st ed., Wiley-VCH, New York.
46. Katz, B. A., Finer-Moore, J., Mortezaei, R., Rich, D. H., and Stroud, R. M. (1995) Episelection: novel Ki approximately nanomolar inhibitors of serine proteases selected by binding or chemistry on an enzyme surface, *Biochemistry* 34, 8264–8280.
47. Groll, M., Berkers, C. R., Ploegh, H. L., and Ova, H. (2006) Crystal structure of the boronic acid-based proteasome inhibitor bortezomib in complex with the yeast 20S proteasome, *Structure* 14, 451–456.
48. Pei, X. Y., Dai, Y., and Grant, S. (2003) The proteasome inhibitor bortezomib promotes mitochondrial injury and apoptosis induced by the small molecule Bcl-2 inhibitor HA14-1 in multiple myeloma cells, *Leukemia* 17, 2036–2045.
49. Ling, Y. H., Liebes, L., Zou, Y., and Perez-Soler, R. (2003) Reactive oxygen species generation and mitochondrial dysfunction in the apoptotic response to bortezomib, a novel proteasome inhibitor, in human H460 non-small cell lung cancer cells, *J. Biol. Chem.* 278, 33714–33723.

BI7002789